

# 鳥取大学研究成果リポジトリ

## Tottori University research result repository

タイトル Title	Self-assembled Artificial Viral Capsid Decorated with Gold Nanoparticles
著者 Author(s)	Matsuura, Kazunori; Ueno, Genki; Fujita, Seiya
掲載誌・巻号・ページ Citation	Polymer journal , 47 (2) : 146 - 151
刊行日 Issue Date	2015
資源タイプ Resource Type	学術雑誌論文 / Journal Article
版区分 Resource Version	著者版 / Author
権利 Rights	注があるものを除き、この著作物は日本国著作権法により保護されています。 / This work is protected under Japanese Copyright Law unless otherwise noted.
DOI	<a href="https://doi.org/10.1038/pj.2014.99">10.1038/pj.2014.99</a>
URL	<a href="http://repository.lib.tottori-u.ac.jp/5724">http://repository.lib.tottori-u.ac.jp/5724</a>

# **Self-assembled Artificial Viral Capsid Decorated with Gold Nanoparticles**

Kazunori Matsuura,<sup>1\*</sup> Genki Ueno,<sup>1</sup> Seiya Fujita<sup>1</sup>

<sup>1</sup> *Department of Chemistry and Biotechnology, Graduate School of Engineering, Tottori University, Koyama-Minami 4-101, Tottori 680-8552, Japan*

Corresponding Author, Fax: +81-857-31-6729; Tel: +81-857-31-5262;

E-mail: ma2ra-k@chem.tottori-u.ac.jp

*Running Head: Gold Nanoparticle-decorated Artificial Viral Capsid*

*Keywords: Self-assembly / Peptide / Spherical virus / Gold nanoparticles / Decoration*

## **Abstract**

The decoration of a peptide-based artificial viral capsid with gold nanoparticles (AuNPs) is reported.  $\beta$ -Annulus GGGCG-bearing peptide as a binding site of AuNPs self-assembled into nanocapsules with a diameter of 50 nm. The addition of AuNPs to the peptide nanocapsules afforded relatively uncontrolled assemblies of AuNPs. In contrast, the self-assembly of AuNP-peptide conjugates afforded, after dialysis, controlled assemblies of AuNPs with sizes of 30–60 nm.  $\zeta$ -Potential measurements revealed that the surface of the artificial viral capsid self-assembled from  $\beta$ -annulus peptide was coated with AuNPs.

## **INTRODUCTION**

Fusion materials of gold nanoparticles (AuNPs) and biomacromolecules have attracted much attention because these materials provide versatile tools for use in applications such as catalysis, biosensing, and bioimaging systems.<sup>1-4</sup> AuNPs have useful electronic, optical, and plasmonic properties, which depend on the diameter of the nanoparticles and the structure of the assemblies. To date, the spatial arrangement of AuNP assemblies has been achieved via the programmed self-assembly of biomacromolecules such as DNA.<sup>5-13</sup> For example, Shultz et al. demonstrated that

oligodeoxyribonucleotide (ODN) conjugates with tethered AuNPs could be arranged by hybridization with the complementary ODN templates.<sup>8,9</sup> Seeman et al. reported that a two-dimensional arrangement of AuNPs with nanosized precision was achieved by the self-assembly of double-crossover DNAs.<sup>10,11</sup>

Natural viral capsids are also attractive biomolecular nanomaterials. Because viral capsids are protein assemblies with a discrete size, space, and a specific aggregation number, they have been used as nanoreactors and nanocontainers for inorganic materials, drugs, and proteins.<sup>14-17</sup> The surface of viral capsids have been utilized as a scaffold to display biomolecular ligands such as saccharides, DNA aptamers, and antigens.<sup>14-17</sup> The regular arrangement of AuNPs on the surface of spherical viral capsids have also been reported.<sup>18-23</sup> Finn et al. demonstrated that monomaleimide-AuNPs were displayed on the surface of Cys-mutated cowpea mosaic virus (CPMV) with a diameter of 30 nm.<sup>18</sup> Blum et al. reported that 5 nm AuNPs were regularly arranged on GGCGG loops inserted into subunit proteins of CPMV.<sup>19-21</sup> Niikura et al. reported the arrangement of sialic-acid-modified AuNPs on JC viral capsids through molecular recognition.<sup>22</sup>

The rational design of self-assembled peptides has been progressively developed for the construction of peptide-based nano-architectures.<sup>24-28</sup> The linear arrangement of AuNPs on fibrous assemblies of peptides has also been reported.<sup>29-31</sup> However, the

literature contains no reports on the spherical arrangement of AuNPs using a rationally designed peptide assembly as a template. Recently, we demonstrated that the designed 24-mer peptide fragment (INHVGGTGGAIMAPVAVTRQLVGS), which participates in the  $\beta$ -annulus motif in tomato bushy stunt virus (TBSV), self-assembles into virus-like nanocapsules with sizes of 30–50 nm.<sup>32-35</sup> Herein, we report the construction of an artificial viral capsid decorated with AuNPs, which we examined using the following two methods: (1) modification of the surface of peptide nanocapsules self-assembled from  $\beta$ -annulus-GGGCG peptide **1** (INHVGGTGGAIMAPVAVTRQLVGSGGGCG) with AuNPs and (2) self-assembly of AuNP- $\beta$ -annulus-GGGCG peptide **1** conjugates (Figure 1).

## **MATERIALS and METHODS**

Reagents were obtained from commercial sources and used without further purification. A stabilized suspension of AuNPs in citrate buffer (5 nm diameter,  $5.5 \times 10^{13}$  particles/mL) was purchased from SIGMA-ALDRICH. Reversed-phase HPLC was performed at ambient temperature on a Shimadzu LC-6AD liquid chromatograph equipped with a UV-vis detector (220 nm, Shimadzu SPD-20A) and GL Science Inertsil WP300 C18 ( $4.6 \times 250$  mm<sup>2</sup> and  $20 \times 250$  mm<sup>2</sup>) columns. MALDI-TOF mass

spectra were obtained on an Autoflex II (Bruker Daltonics) spectrometer operated under the linear/positive mode with  $\alpha$ -cyano-4-hydroxy cinnamic acid ( $\alpha$ -CHCA) as the matrix. UV-vis spectra were recorded at 25°C using a JASCO V-630 spectrophotometer. CD spectra were collected in a 1-mm quartz cell with a JASCO J-820 spectrophotometer at 25°C. Molar concentrations of AuNPs were calculated using the absorbance at 520 nm.

**Synthesis of peptide (1).** The peptide H-Ile-Asn(Trt)-His-(Trt)-Val-Gly-Gly-Thr(tBu)-Gly-Gly-Ala-Ile-Met-Ala-Pro-Val-Ala-Val-Thr(tBu)-Arg(pbf)-Gln(Trt)-Leu-Val-Gly-Ser(tBu)-Gly-Gly-Gly-Cys(Trt)-Gly-Alko-PEG resin was synthesized on a Fmoc-Gly-Alko-PEG resin (Watanabe Chemical Ind., Ltd., 0.22 mmol/g) using Fmoc-based coupling reactions (4 equiv. Fmoc amino acids). Solutions of 2-(1*H*-benzotriazole-1-yl)-1,1,3,3-tetramethyluronium hexafluorophosphate (HBTU, 4 equiv.), 1-hydroxybenzotriazole hydrate (HOBt•H<sub>2</sub>O, 4 equiv.), and diisopropylamine (8 equiv.) in *N*-methylpyrrolidone (NMP) were used as coupling reagents. A solution of 20 % piperidine in *N,N*-dimethylformamide (DMF) was used for Fmoc deprotection. The progress of the coupling reaction and Fmoc deprotection was confirmed using a TNBS and a Chloranil Test Kit (Tokyo Chemical Industry Co., Ltd.). The peptidyl resin was washed with NMP.

The peptide was deprotected and cleaved from the resin by treatment with a mixture of trifluoroacetic acid (TFA)/water/1,2-ethanedithiol/triisopropylsilane = 9.5/0.25/0.25/0.1 at room temperature for 3 h. The reaction mixture was filtered to remove the resin and the filtrate was concentrated under vacuum. The peptide was precipitated by the addition of methyl *tert*-butyl ether (MTBE) to the residue, and the supernatant was decanted. After the peptide was washed with MTBE three times, the precipitated peptide was dried under vacuum. The crude product was purified by reversed-phase HPLC (Inertsil WP300 C18), eluting with a linear gradient of CH<sub>3</sub>CN/water containing 0.1% TFA (26/74 to 29/71 over 120 min). The fraction containing the desired peptide was lyophilized to give 9.5 mg of a flocculent solid (3 % yield). MALDI-TOF-MS (matrix:  $\alpha$ -CHCA):  $m/z = 2638 [M+H]^+$ .

**Modification of the surface of peptide nanocapsules with AuNPs.** An aqueous solution of  $\beta$ -annulus-GGGCG peptide **1** (0.2 mM, pH 4.6) was prepared by simply dissolving it in deionized water. The formation of spherical assemblies was confirmed by dynamic light scattering (DLS) measurements and transmission electron microscopy (TEM). The aqueous solution of peptide **1** (37.5  $\mu$ L) was mixed with AuNPs in citrate buffer ( $5.5 \times 10^{13}$  particles/mL, 30  $\mu$ L) and incubated for 60 min at 25°C. An aliquot (7.5  $\mu$ L) of 20 mM thioctic acid solution in ethanol/water (4/1) was added to the

mixture of peptide **1** and gold nanoparticles, and the resulting mixture was incubated for 10 min at 25°C. The final concentrations were [peptide **1**] = 0.1 mM, [AuNP] = 0.2 μM, and [thioctic acid] = 2 mM (pH of the final solution was 3.7).

**Construction of artificial viral capsid decorated with AuNPs by self-assembly of**

**AuNP–peptide conjugates.** An aqueous solution of β-annulus-GGGCG peptide **1** was

diluted with water to a concentration of 2 μM, which is less than the critical aggregation

concentration. An aliquot (2 mL) of the aqueous solution of peptide **1** (2 μM) was

mixed with a diluted AuNPs dispersion ([AuNP] = 1 μM, 2 mL) and incubated for 60

min at 25°C. An aliquot (0.5 mL) of 20 mM thioctic acid solution in ethanol/water (4/1)

was added to the mixture of peptide **1** and AuNPs, and the resulting mixture was

incubated for 10 min at 25°C. The water in the mixture was evaporated using a Smart

Evaporator<sup>®</sup> (Bio Chromato, Inc.). The residue was redispersed by the addition of water

(80 μL) to final concentrations of [peptide **1**] = 50 μM and [AuNP] = 25 μM. To remove

unassembled AuNPs, peptides, and AuNP–peptide conjugates, the dispersion of

AuNP–peptide conjugates was dialyzed to equilibrium against water using Spectra/Por<sup>®</sup>

dialysis tubing (cutoff Mw = 50 kDa, Spectrum Laboratories, Inc.). Nanostructures of

the assemblies were evaluated by DLS measurements and TEM observations.

**Dynamic light scattering (DLS) measurements.** DLS measurements were performed



using a Zetasizer NanoZS (MALVERN Instruments, Ltd.) instrument at 25 °C with an incident He–Ne laser (633 nm). During the measurements, the count rate (the sample-scattering intensity) was also provided. The correlation time for the scattered light intensity  $G(\tau)$  was measured several times, and the averaged results were fitted to equation 1:

$$G(\tau) = B + A \exp(-2q^2D\tau) \quad (1)$$

where  $B$  is the baseline,  $A$  is the amplitude,  $q$  is the scattering vector,  $\tau$  is the delay time, and  $D$  is the diffusion coefficient. The hydrodynamic radius ( $R_H$ ) of the scattering particles was calculated using the Stokes–Einstein equation (eq. 2):

$$R_H = \frac{k_B T}{6\pi\eta D} \quad (2)$$

where  $\eta$  is the solvent viscosity,  $k_B$  is Boltzmann's constant and  $T$  denotes the absolute temperature.

**$\zeta$ -Potential measurements.** We determined the  $\zeta$ -potential of peptide assemblies at pH 4.6 by measuring the electrophoretic mobility at 25 °C in disposable Zeta cells using a Zetasizer NanoZS (MALVERN Instruments, Ltd.).

**Transmission electron microscopy (TEM).** An aliquot (5  $\mu$ L) of each sample solution was applied to a carbon-coated grid (ALLANCE Biosystems), left for 60 s,

and then removed. The grid was subsequently dried in vacuo. In the case of peptide samples, a drop of 2 wt% aqueous sodium phosphotungstate was placed on each of the grids. AuNPs were observed without the use of a stain. After the sample-loaded carbon-coated grids were dried in vacuo, they were observed by TEM (JEOL JEM 1400 Plus) using an acceleration voltage of 80 kV.

## **RESULTS and DISCUSSION**

29-mer  $\beta$ -annulus-GGGCG peptide **1** (INHVGGTGGAIMAPVAVTRQLVGS GGGCG) was synthesized using the Fmoc-protected solid-phase method, purified by reversed-phase HPLC, and confirmed by MALDI-TOF-MS ( $m/z = 2637$  [M]<sup>+</sup>). The CD spectrum of the aqueous solution of peptide **1** showed a negative peak at 202 nm and a negative shoulder at approximately 220–230 nm (Figure 2a), which is similar to the CD spectrum of a 24-mer  $\beta$ -annulus peptide reported previously,<sup>32</sup> indicating the coexistence of random-coil,  $\beta$ -sheet, and turn structures. DLS measurement of the aqueous solution of peptide **1** showed that peptide **1** formed assemblies with a hydrodynamic diameter of  $51 \pm 15$  nm (Figure 2b). TEM observation of the assemblies stained with sodium phosphotungstate also showed the formation of spherical structures with a diameter of approximately 50 nm (Figure 2c), which is

comparable to the size (30–50 nm) of nanocapsules self-assembled from 24-mer  $\beta$ -annulus peptide.<sup>32</sup> The concentration dependence of peptide **1** on the scattering intensity (DLS count rate) revealed that the critical aggregation concentration (CAC) at 25°C is 29  $\mu$ M, which is comparable to the CAC (25  $\mu$ M) of 24-mer  $\beta$ -annulus peptide under the same conditions.<sup>32</sup> These results indicate that the addition of GGGCG to the terminus of the  $\beta$ -annulus peptide minimally affected the size, morphology, and stability of the spherical peptide assemblies.

To construct artificial viral capsids decorated with AuNPs, an aqueous dispersion of AuNPs was added to the aqueous dispersion of nanocapsules self-assembled from  $\beta$ -annulus-GGGCG peptide **1**, and then the surface of the AuNPs was subsequently protected with thioctic acid to prevent further aggregation (Figure 1a). When a suspension of 0.2  $\mu$ M AuNPs was mixed with 0.1 mM peptide **1**, the TEM micrographs of the product showed the formation of spherical assemblies with a diameter of 10–50 nm and which comprised 2–40 AuNPs with a diameter of 5 nm (Figure 3a). In contrast, the TEM micrographs of AuNPs in the absence of peptide **1** showed only individually-dispersed AuNPs (Figure S1). The DLS of the mixture of AuNPs and peptide **1** also showed the formation of assemblies with a hydrodynamic diameter of  $60 \pm 19$  nm (Figure 3b). The UV–vis spectrum of AuNPs in the

presence of the peptide nanocapsule was slightly red-shifted (Figure 3c), which is ascribed to plasmon coupling among AuNPs self-assembled on the peptide nanocapsule. Notably, assemblies of AuNPs were observed, although the concentration of AuNPs was remarkably smaller than that of peptide **1**. Niikura et al. reported the cooperative binding of sialic-acid-modified AuNPs on JC viral capsid.<sup>22</sup> In the present study, the AuNPs apparently cooperatively adsorbed onto Cys residues at the surface of the peptide nanocapsules. However, assemblies consisting of several AuNPs were also observed in the TEM micrographs (Figure 3a); therefore, controlling the aggregation number of AuNPs on a peptide nanocapsule is difficult with this method.

Next, we examined the construction of artificial viral capsid decorated with AuNPs by the self-assembly of AuNP–peptide **1** conjugates (Figure 1b). We mixed AuNPs with a diluted solution of  $\beta$ -annulus-GGGCG peptide **1** at a concentration below the CAC to prepare their conjugate and then protected the surface of the AuNPs with thiocetic acid. The solvent in the dispersion of conjugate was evaporated, and the conjugate was subsequently redispersed in water to final concentrations of [peptide **1**] = 50  $\mu$ M and [AuNP] = 25  $\mu$ M. The TEM images of the dispersion of AuNP–peptide **1** conjugates showed the coexistence of AuNP assemblies with a

diameter of 30–50 nm and unassembled AuNPs (Figure 4a). After the unassembled AuNPs were removed using a dialysis membrane (cutoff  $M_w = 50$  kDa), AuNP assemblies with diameters of 30–60 nm were selectively observed in the TEM images (Figure 4b). The DLS of the dialyzed dispersion of AuNP–peptide **1** conjugates also indicated the formation of assemblies with a hydrodynamic diameter of  $76 \pm 25$  nm (Figure 4b). The assemblies observed by TEM consisted of 22–63 AuNPs, which partially corresponds to the ideal aggregation number of 60 for a dodecahedral peptide assembly. The increase in diameter compared with that of unmodified peptide nanocapsules ( $51 \pm 15$  nm, Figure 2b) suggests that AuNPs decorate the surface of the peptide nanocapsules. The UV–vis spectrum of the assembly of AuNP–peptide **1** conjugates was approximately the same as that of individual AuNPs (Figure 4c), which indicates that the AuNPs are separated from one another on the peptide nanocapsules. The difference between hydrodynamic diameters obtained from DLS before and after dialysis (Figure 4a and 4b) might be caused by pH change of the solutions (The pH before dialysis was 3.7, but that after dialysis was 4.6).

As previously reported,<sup>34</sup> the pH dependence of the  $\zeta$ -potential of peptide nanocapsules self-assembled from  $\beta$ -annulus peptide indicates that the C-termini are

directed toward the exterior of the peptide nanocapsules. Therefore, we expected that Cys residues of  $\beta$ -annulus-GGGCG peptide **1** and AuNPs are directed toward the exterior of the peptide nanocapsules. The  $\zeta$ -potential of unmodified peptide nanocapsules was approximately neutral ( $0.01 \pm 3.43$  mV) at pH 4.6 (Figure 5a). In contrast, the  $\zeta$ -potential of the assemblies of AuNP–peptide **1** conjugates was  $-30.5 \pm 9.8$  mV at pH 4.6 (Figure 5b), corresponding to that of AuNP dispersion in citrate buffer ( $-30.0 \pm 12$  mV, Figure S1). These results clearly indicate that the surface of artificial viral capsid self-assembled from  $\beta$ -annulus peptide was coated with AuNPs.

## CONCLUSION

We demonstrated that AuNP (5 nm)- $\beta$ -annulus-GGGCG peptide self-assembled to afford artificial viral capsids decorated with AuNPs. The AuNP-modified viral capsids could be applied as scattering imaging capsules in cells.<sup>36</sup> The present strategy extends the design of artificial viral capsids to include decoration with other functional molecules such as proteins, DNA, and fluorophores.

## **Acknowledgements**

This research was partially supported by a Grant-in-Aid for Scientific Research on the Innovative Areas of “Fusion Materials” (No. 2206) from the Ministry of Education, Science, Sports and Culture of Japan (MEXT) and by the Asahi Glass Foundation.

## **References**

- 1 Louis C. & Pluchery, O. *Gold nanoparticles for physics, chemistry and biology* (Imperial College Press, London, 2012).
- 2 Daniel, M.-C. & Astruc, D. Gold Nanoparticles: Assembly, supramolecular chemistry, quantum-size-related properties, and applications toward biology, catalysis, and nanotechnology. *Chem. Rev.* **104**, 293–346 (2004).
- 3 Sperling, R. A., Gil, P. R., Zhang, F., Zanella M., & Parak, W. J. Biological applications of gold nanoparticles. *Chem. Soc. Rev.* **37**, 1896–1908 (2008).
- 4 Saha, K., Agasti, S. S., Kim, C., Li, X., & Rotello, V. M. Gold nanoparticles in chemical and biological sensing. *Chem. Rev.* **112**, pp 2739–2779 (2012).
- 5 Gothelf, K. V. & LaBean, T. H. DNA-programmed assembly of nanostructures. *Org. Biomol. Chem.* **3**, 4023–4037 (2005).

- 6 Kuzuya A. & Ohya Y. DNA nanostructures as scaffolds for metal nanoparticles. *Polymer J.* **44**, 452–460 (2012).
- 7 Mirkin, C. A., Letsinger, R. L., Mucic, R. C., & Storhoff, J. J. A DNA-based method for rationally assembling nanoparticles into macroscopic materials. *Nature* **382**, 607–609 (1996).
- 8 Alivisatos, A. P., Johnsson, K. P., Peng, X., Wilson, T. E., Loweth, C. J., Bruchez, M. P., Jr., & Schultz, P. G. Organization of 'nanocrystal molecules' using DNA. *Nature* **382**, 609–611 (1996).
- 9 Loweth, C. J., Caldwell, W. B., Peng, X., Alivisatos, A. P., & Schultz, P. G. DNA-based assembly of gold nanocrystals. *Angew. Chem. Int. Ed.* **38**, 1808–1812 (1999).
- 10 Le, J. D., Pinto, Y., Seeman, N. C., Musier-Forsyth, K., Taton, T. A. & Kiehl, R. A. DNA-templated self-Assembly of metallic nanocomponent arrays on a surface. *Nano Lett.* **4**, 2343–2347 (2004).
- 11 Zheng, J., Constantinou, P. E., Micheel, C., Alivisatos, A. P., Kiehl, R. A., & Seeman, N. C. Two-dimensional nanoparticle arrays show the organizational power of robust DNA motifs. *Nano Lett.* **6**, 1502–1504 (2006).
- 12 Mastroianni, A. J., Claridge, S. A., & Alivisatos, A. P. Pyramidal and chiral



- groupings of gold nanocrystals assembled using DNA scaffolds. *J. Am. Chem. Soc.* **131**, 8455–8459 (2009).
- 13 Tamaki, T., Miyoshi, N., Uehara, T., & Ohya, Y. Isolation of gold nanoparticle/oligo-DNA conjugates by the number of oligo-DNAs attached and their formation of self-assembly. *Chem. Lett.* **39**, 1084–1085 (2010).
- 14 Douglas, T. & Young, M. Viruses: Making friends with old foes. *Science* **312**, 873–875 (2006).
- 15 Steinmetz, N. F. & Evans, D. J. Utilisation of plant viruses in bionanotechnology. *Org. Biomol. Chem.* **5**, 2891–2902 (2007).
- 16 Bronstein, L. M. Virus-based nanoparticles with inorganic cargo: What does the future hold? *Small* **7**, 1609–1618 (2011).
- 17 Witus, L. S. & Francis, M. B. Using synthetically modified proteins to make new materials. *Acc. Chem. Res.* **44**, 774–783 (2011).
- 18 Wang, Q., Lin, T., Tang, L., Johnson, J. E., & Finn, M. G. Icosahedral virus particles as addressable nanoscale building blocks. *Angew. Chem. Int. Ed.* **41**, 459–462 (2002).
- 19 Blum, A. S., Soto, C. M., Wilson, C. D., Cole, J. D., Kim, M., Gnade, B., Chatterji, A., Ochoa, W. F., Lin, T. W., Johnson, J. E., & Ratna, B. R. Cowpea

- mosaic virus as a scaffold for 3-D patterning of gold nanoparticles. *Nano Lett.* **4**, 867–870 (2004).
- 20 Blum, A. S., Soto, C. M., Wilson, C. D., Brower, T. L., Pollack, S. K., Schull, T. L., Chatterji, A., Lin, T., Johnson, J. E., Amsinck, C., Franzon, P., Shashidhar, R., & Ratna, B. R. An engineered virus as a scaffold for three-dimensional self-assembly on the nanoscale. *Small* **1**, 702–706 (2005).
- 21 Soto, C. M., Blum, A. S., Wilson, C. D., Lazorcik, J., Kim, M., Gnade, B. & Ratna, B. R. Separation and recovery of intact gold-virus complex by agarose electrophoresis and electroelution: Application to the purification of cowpea mosaic virus and colloidal gold complex. *Electrophoresis* **25**, 2901–2906 (2004).
- 22 Niikura, K., Nagakawa, K., Ohtake, N., Suzuki, T., Matsuo, Y., Sawa, H., & Ijiro, K. Gold nanoparticle arrangement on viral particles through carbohydrate recognition: A non-cross-linking approach to optical virus detection. *Bioconj. Chem.* **20**, 1848–1852 (2009).
- 23 Nagakawa, K., Niikura, K., Suzuki, T., Matsuo, Y., Igarashi, Y., Sawa, H., & Ijiro, K. Virus capsid coating of gold nanoparticles via cysteine-Au interactions and their effective cellular uptakes. *Chem. Lett.* **41**, 113–115 (2012).

- 24 Matsuura, K. Rational design of self-assembled proteins and peptides for nano- and micro-sized architectures. *RSC Adv.* **4**, 2942–2953 (2014).
- 25 Ramakers, B. E. I., van Hest, J. C. M., & Lowik, D. Molecular tools for the construction of peptide-based materials. *Chem. Soc. Rev.* **43**, 2743–2756 (2014).
- 26 Boyle, A. L., Bromley, E. H. C., Bartlett, G. J., Sessions, R. B., Sharp, T. H., Williams, C. L., Curmi, P. M. G., Forde, N. R., Linke, H. & Woolfson D. N. Squaring the circle in peptide assembly: From fibers to discrete nanostructures by de novo design. *J. Am. Chem. Soc.*, **134**, 15457–15467 (2012).
- 27 Fletcher, J. M., Harniman, R. L., Barnes, Fr. R. H., Boyle, A. L., Collins, A., Mantell, J., Sharp, T. H., Antognozzi, M., Booth, P. J., Linden, N., Miles, M. J., Sessions, R. B., Verkade, P., & Woolfson, D. N. Self-assembling cages from coiled-coil peptide modules. *Science*, **340**, 595–599 (2013).
- 28 H. Gradišar, S. Božič, T. Doles, D. Vengust, I. Hafner-Bratkovič, A. Mertelj, B. Webb, A. Šali, S. Klavžar and R. Jerala, Design of a single-chain polypeptide tetrahedron assembled from coiled-coil segments. *Nat. Chem. Biol.*, 2013, **9**, 362–366.
- 29 Ryadnov, M. G., Ceyhan, B., Niemeyer, C. M., & Woolfson, D. N. “Belt and braces”: A peptide-based linker system of de novo design. *J. Am. Chem. Soc.*

**125**, 9388–9394 (2003).

30 Sawada, T., Takahashi, T., & Mihara, H. Affinity-based screening of peptides recognizing assembly states of self-assembling peptide nanomaterials. *J. Am. Chem. Soc.* **131**, 14434–14441 (2009).

31 Nonoyama, T., Tanaka, M., Inai, Y., Higuchi, M., & Kinoshita T. Ordered nanopattern arrangement of gold nanoparticles on  $\beta$ -sheet peptide templates through nucleobase pairing. *ACS Nano* **5**, 6174–6183 (2011).

32 Matsuura, K., Watanabe, K., Sakurai, K., Matsuzaki, T., & Kimizuka, N. Self-assembled synthetic viral capsids from a 24-mer viral peptide fragment. *Angew. Chem. Int. Ed.* **49**, 9662–9665 (2010).

33 Matsuura, K. Construction of spherical virus-inspired peptide nanoassemblies. *Polymer J.*, **44**, 469–474 (2012).

34 Matsuura, K., Watanabe, K., Matsushita, Y., Kimizuka, N. Guest-binding behavior of peptide nanocapsules self-assembled from viral peptide fragments. *Polymer. J.* **45**, 529–534 (2013).

35 Fujita, S. & Matsuura, K. Inclusion of zinc oxide nanoparticles into virus-like peptide nanocapsules self-assembled from viral  $\beta$ -annulus peptide. submitted to *Nanomaterials*.

36 Wan, X., Zheng, L., Gao, P., Yang, X., Li, C., Li, Y. F., & Huang C. Z.

Real-time light scattering tracking of gold nanoparticles-bioconjugated respiratory syncytial virus infecting HEp-2 cells. *Sci. Rep.* **4**, 4529 (2014).

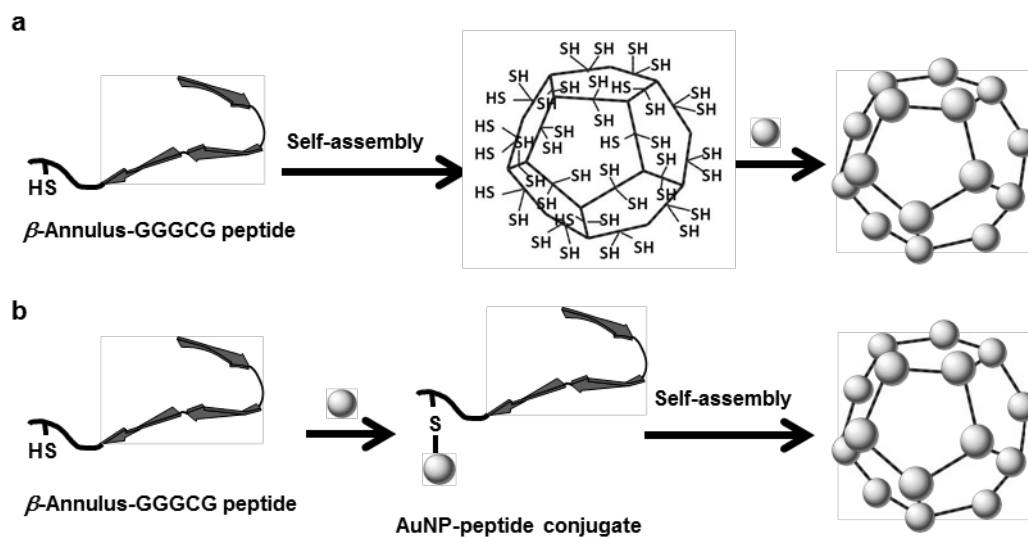


**Figure 1** Schematic of an artificial viral capsid decorated with gold nanoparticles. a) Modification of the peptide nanocapsules self-assembled from  $\beta$ -annulus-GGGCG peptide **1** with AuNPs. b) Self-assembly of AuNP- $\beta$ -annulus-GGGCG peptide **1** conjugates.

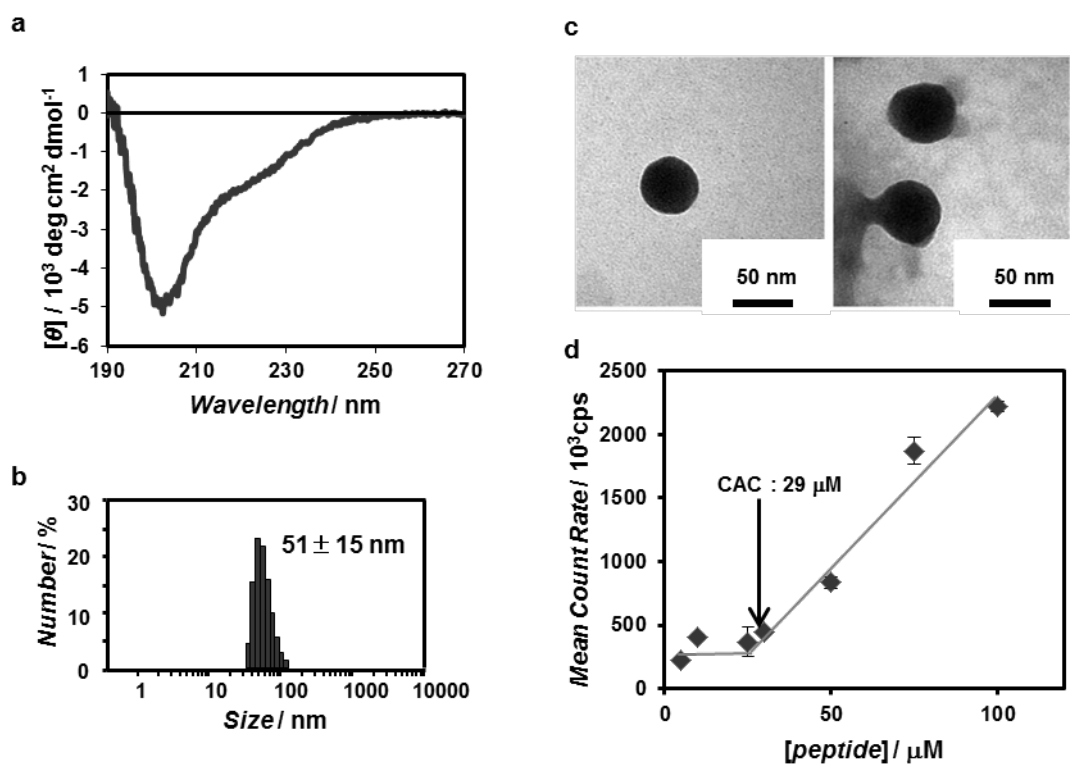


**Figure 2** (a) CD spectrum of an aqueous solution of  $\beta$ -annulus-GGGCG peptide (0.1 mM) at 25°C. (b) Size distribution of an aqueous solution of  $\beta$ -annulus-GGGCG peptide (0.1 mM) determined at 25°C by DLS. (c) TEM image of the assemblies obtained from an aqueous solution of  $\beta$ -annulus-GGGCG peptide (0.1 mM). The TEM sample was stained with 2% phosphotungstic acid. (d) Effect of peptide concentration on scattering intensity determined at 25°C by DLS.

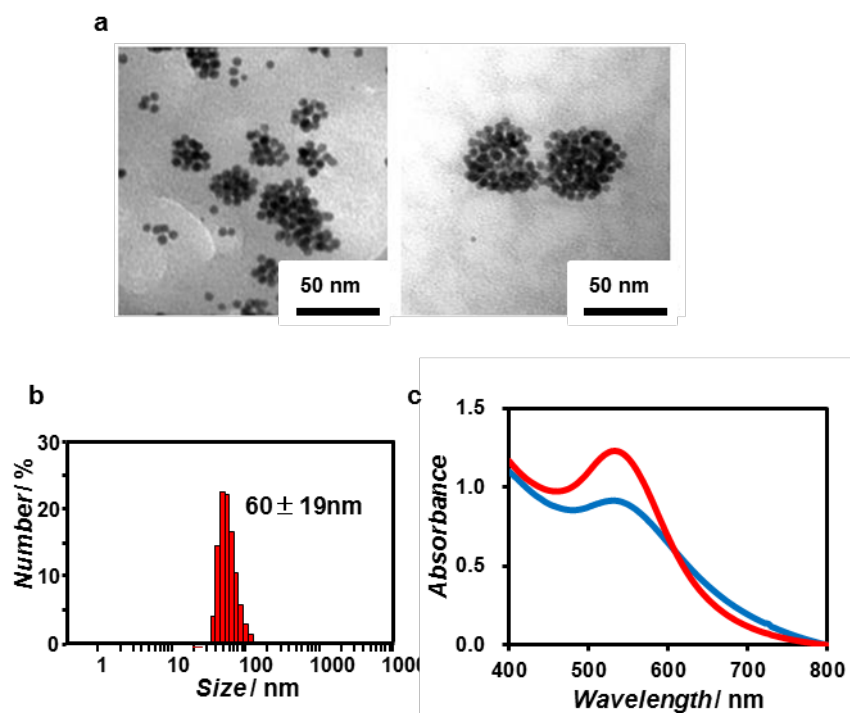


**Figure 3** (a) TEM images of AuNPs ( $0.2 \mu\text{M}$ ) mixed with the peptide nanocapsules ( $[\text{peptide } \mathbf{1}] = 0.1 \text{ mM}$ ). (b) Size distribution of assembly of AuNPs ( $0.2 \mu\text{M}$ ) mixed with the peptide nanocapsules ( $[\text{peptide } \mathbf{1}] = 0.1 \text{ mM}$ ) determined at  $25^\circ\text{C}$  by DLS. (c) UV-vis spectra of aqueous dispersion of AuNP (red) at  $0.1 \mu\text{M}$  and the assembly of AuNPs ( $0.1 \mu\text{M}$ ) mixed with the peptide nanocapsules ( $[\text{peptide } \mathbf{1}] = 0.05 \text{ mM}$ ) (blue) at  $25^\circ\text{C}$ .



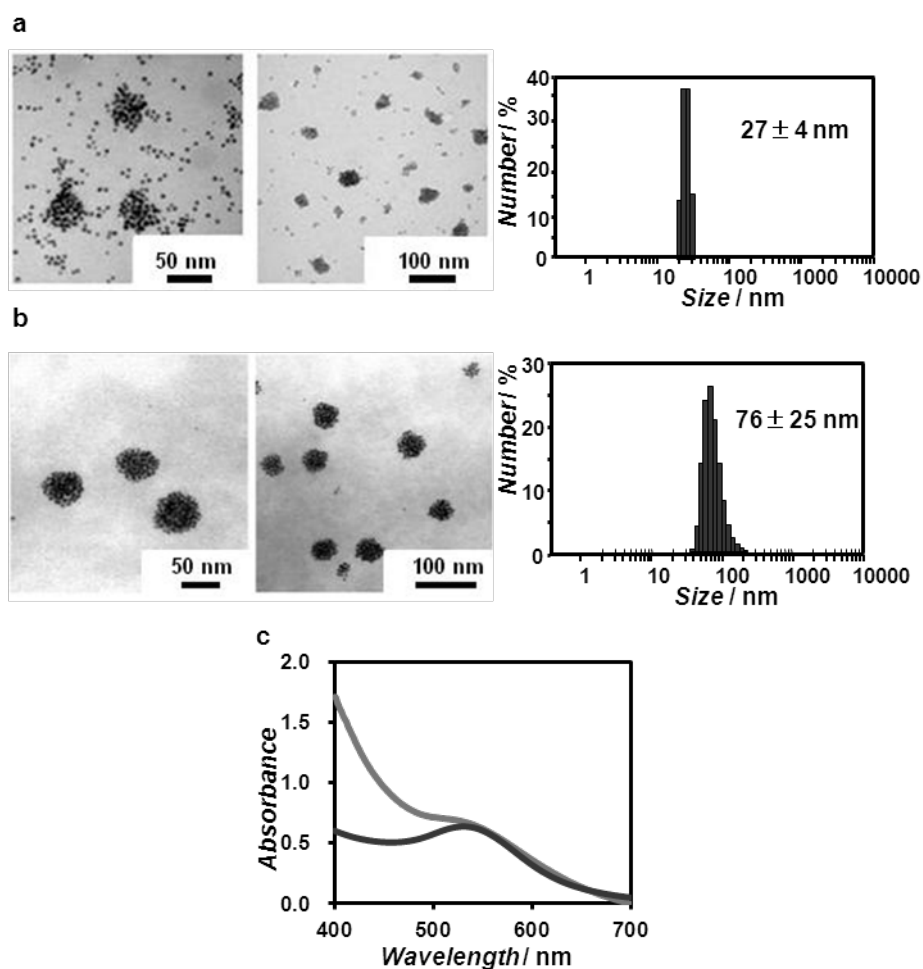


**Figure 4** TEM images and size distribution of assemblies of AuNP-peptide conjugates by DLS before (a) and after (b) dialysis at 25°C ([peptide] = 50  $\mu$ M, [AuNP] = 25  $\mu$ M). (c) UV-vis spectra of a diluted aqueous dispersion of AuNP (black) and an artificial viral capsid decorated with gold nanoparticles after dialysis (gray) at 25°C. The concentration of AuNPs after dialysis was calculated to be 0.06  $\mu$ M.

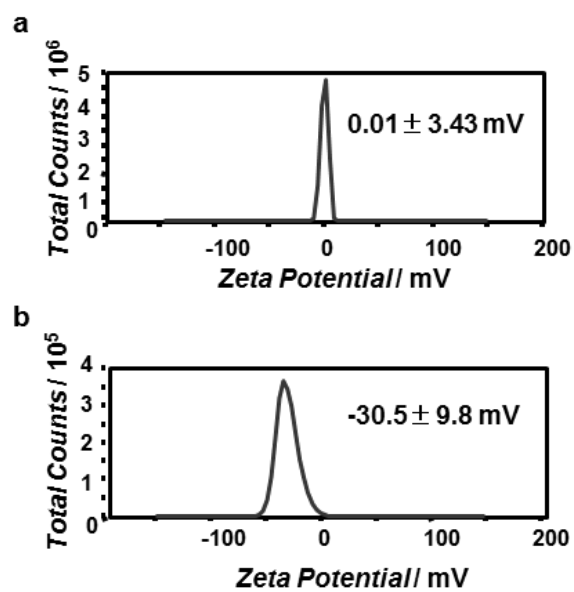


**Figure 5** Zeta potentials of (a)  $\beta$ -annulus-GGGCG peptide **1** (0.1 mM) and (b) artificial viral capsid decorated with gold nanoparticles after dialysis in water at pH 4.6 and at 25°C.

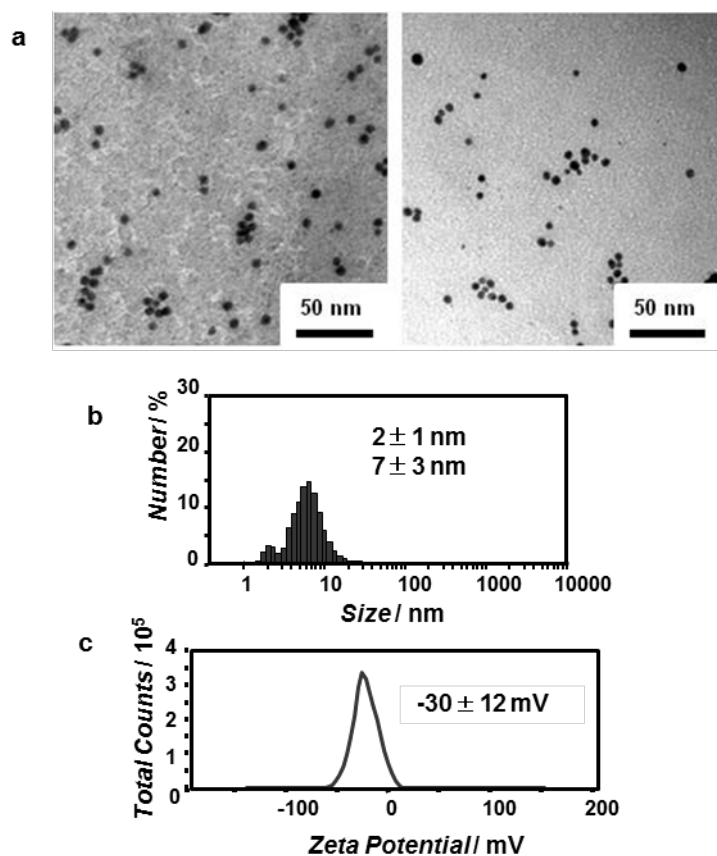


**Figure S1** (a) TEM images, (b) size distribution determined by DLS, and (c) zeta potential of AuNP dispersion in citrate buffer.